INLAND FOREST MODEL DESIGN CONSIDERING TSUNAMI BORNE LARGE DRIFTWOOD

ROWAN SACHIKA DE COSTA
Doctoral Student. Graduate School of Science and Engineering, Saitama University, Saitama, Japan SachikaDeCosta@hotmail.com

NORIO TANAKA
Professor, International Institute for Resilient Society, Saitama University, Saitama, Japan tanaka01@mail.saitama-u.ac.jp

ABSTRACT

An inland forest can be used to not only dampen the impact by a tsunami but also prevent impact by tsunami borne driftwood, by trapping them within a forest. This paper hopes to develop the understanding of an inland forest model (IFM) by elucidating the trapping function of an IFM and the effect of trapped driftwood on the incoming flow. Variables of an IFM include spacings between the tree trunks (*G*/*D*; gap between cylinders/ diameter of the cylinder; cylinder representing the trunks of the tree), number of rows and the initial Froude number (*Fr*) (Initial being the flow condition when no IFM exist). Two different laboratory experiments were conducted using a small coniferous plant. The first experiment elucidated the effect of tsunami borne large driftwood (TLD) angle against the streamlines and the trapping function of an IFM with *G*/*D* ratios of 10.6, 6.8 and 3.0. It showed that TLD that attacks an IFM in a cross-stream position increased the trapping function of an IFM than the TLD being in a streamwise position, an additional increase of 20% in *G*/*D* of 6.8. The second experiment showed that the *G*/*D* ratio of 4.53 had a different trapping pattern than a *G*/*D* ratio of 0.88. Therefore, the effect of trapped TLD on the incoming flow was different. The *G*/*D* ratio of 4.53 showed an approximately 5% decrease to the downstream flow.

Keywords: Disaster prevention engineering, Driftwood management, Inland forest design, Tsunami mitigation, Trapping of driftwood

1. INTRODUCTION

Due to a large population that resides near coastal areas establishing resilient methods to mitigate tsunami damage is important (Marois and Mitsch 2015). The use of coastal forests as a tsunami mitigation strategy has gained significant recognition, with field observations and research being conducted throughout the world (De Costa and Nandasena 2018; Tanaka et al. 2018).

Coastal forests, for example, conifers, coconut, and Pohutukawa trees are common coastal trees in Japan, Sri Lanka, and New Zealand, respectively (De Costa and Nandasena 2018; Tanaka et al. 2018). The coastal forest provides a drag force, induce turbulence, and can reflect the wave. These are some of the factors that cause a reduction in flow energy downstream of a forest patch, which means a reduction in the damage caused by a tsunami wave. However, especially noticed in the Sendai region of Japan, trees can be broken (Udo et al. 2012; Tanaka and Suzuki 2013). These damaged trees can create additional point loads or block openings that are required to reduce the hydrostatic and hydrodynamic loading (Tanaka and Suzuki 2013; Tanaka and Onai 2017; Tanaka and Ogino 2017; Stolle et al. 2018). These point loads add to the damage caused by a tsunami, potentially colliding on schools, hospitals, and government buildings. Even though the coastal forest has many positives in tsunami mitigation, the management of tsunami borne large driftwood (TLD) needs to be considered.

Inland forest has shown the capability to trap TLD, and research on encouraging trapping exists (Pasha and Tanaka 2016; Imai et al. 2018; De Costa and Tanaka 2020). Trees are a suitable method because it is natural, tall, and has already shown the capability to trap driftwood. Moreover, it encourages the use of green infrastructure in a society (Natuhara 2018). However, consideration of secondary damage, damage to the inland forest by driftwood, needs to be discussed. Driftwood's impact force depends on factors like velocity, impact geometry, driftwood mass and collision stiffness (Haehnel and Daly 2004; Schmocker and Hager 2013). However, since the trapping forest is inland, the flow has undergone energy dissipation, and the Froude number (*Fr*) has decreased (Tanaka et al. 2014). This means a smaller driftwood velocity and a lower impact height. It is implying a lower chance of the trapping forest from getting damaged. Moreover, due to the trees

growing in the inland region, the groundwater may contain a lesser volume of salts, therefore allowing for stronger roots to grow (Felisa et al. 2013). This all implying that an inland forest (IF), has strong potential to trap TLD safely.

A recent study was conducted to understand a potential method to encourage trapping. De Costa et al. (2019) showed that by placing an embankment followed by a moat structure, the driftwood model rotated against the streamlines. This increased the cross-stream length of the driftwood. This increase in cross-stream length has the potential to increase the trapping function of an IF. Moreover, once a forest patch traps driftwood, it affects to change the incoming flow. Therefore, the objective of this study was to investigate the trapping rate of TLD by an IF. TLD being at different angles to the streamlines, before its impact, and, the effect of a group of TLD trapped by an IFM has to the incoming flow were studies. Additionally, different IFM properties such as the spacing of the trees, the number of rows of trees and varying the *Fr* conditions were investigated. Generally, numerical models do not consider trapped TLDs in front of an IFM, and therefore, this experiment hopes to provide some insight into this. The study hopes to elucidate the trapping function and the effect of trapped TLD by an IF. This study is to make the application of an IF more resilient to a tsunami disaster.

2. MATERIALS AND METHODS

2.1 Understanding trapping function, of a TLD by an IFM given rotated TLD

A similar methodology was conducted to, as explained in (De Costa and Tanaka 2020). The experiment was conducted in a 0.5 m wide, 0.5 m deep, and 14 m long flume channel with a slope of 1/1000 (Figure 1 a)). A flow rate of 0.015 m^3s^{-1} (*Fr* around 0.5) was pumped at a quasi-steady state through the flume channel. It was known numerically and through the 2011 Great East Japan Tsunami that the *Fr* of a tsunami wave 550 m downstream from the shoreline of a thick vegetation patch, was around 0.6, and it decreased as the wave propagated further inland (Tanaka et al. 2014). This flow rate made the driftwood model be in a fully floating condition i.e. the driftwood model was fully buoyant when it was placed on to the flow.

A model scale of 1/20 was chosen for this laboratory experiment. Wooden poles of 0.01 m diameter were used to represent the average trunk diameter of an inland forest model (IFM) in a laboratory experiment. The IFM was assumed to represent inland trapping by the trunk(s) only, and that the influence of the crown in IFM was ignored. Three different spacings (*S*) between the cylinders were considered. They were, 0.221, 0.145 and 0.07 m receptively. The 0.01 m diameter and 0.221 m *S* are model scale distance based on the actual tree diameter and spacing of Guimatsu *(Larix gmelinii* Rupr.*)* in Taiki Town, Hokkaido, Japan (Tanaka et al. 2018). Maintaining the same diameter, *S* 0.07 m was chosen based on the maximum crown width of the driftwood model and *S* 0.145 m was based on the average between 0.221 and 0.07 m. These gave *G*/*D* values (the gap between cylinders/diameter of the cylinder; cylinder representing the trunks of the tree (Takemura and Tanaka 2007)) of 10.6, 6.8 and 3.0, respectively. Three different rows were considered. They were 1, 2 and 3 rows in the IFM, respectively. Thuy et al. (2012) noted that staggering the trunks performed better in reducing the energy as compared to a non-staggered arrangement. Therefore, the rows were placed in a staggered pattern. The centre pole in the first row of the respective IFM was attached to a force gauge (10N force-gauge SSK LB60-10N at a sampling rate of 100Hz), to measure the streamwise impact force against the trunk of a tree.

The driftwood used in the experiment were two model scale conifer plants (*Chamaecyparis lawsoniana*. (A. Murray)), (Figure 1 a) shows one of the two driftwood models used). They were used to represent the broken tree condition (driftwood model without roots). The approximate height of the driftwood models was 0.28 m with an approximate crown width of 0.07 m and a crown height of 0.25 m. All the models used had an oval type crown shape, with the branches facing upwards. Three different trunk height to tree height ratios (H_{ND}; a variable referred from (De Costa and Tanaka 2020)) were considered. They were H_{ND} values of 0.06, 0.12 and 0.18, respectively. While experimenting, the specific gravity of the models used was calculated to be approximately 0.96, which represented well with the actual TLD, specific gravity being around 1 (Tanaka and Ogino 2017).

The driftwood model was released approximately 2 m upstream from the first row of an IFM. The driftwood was released at 0°, 45° and 90° to the streamlines. The average velocity of the driftwood model, for the three respective rotated positions, were, 0.46, 0.47 and 0.49 ms^{-1}. Since rotated driftwood had a higher drag force, a 90° rotated driftwood model had the highest velocity. Each experiment case and for each of the two driftwood models, the experiment was repeated ten times. After the release of the driftwood model, the trapping pattern and force against time were noted and measured. The driftwood was removed from the flume channel. Altogether for each respective scenario, the experiment was repeated twenty times. The driftwood was released in line with the force gauge. The data was then analyzed based on the respective variable being tested [Eq. (1)].

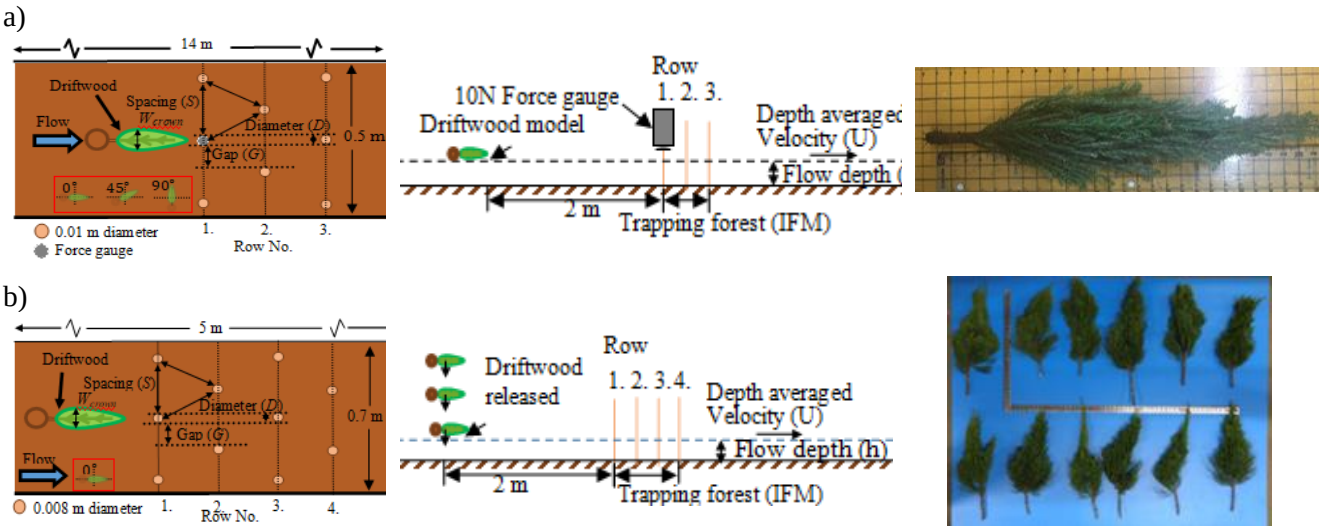

Figure 1: Plan view, side view and the driftwood model used in this experiment; First row of figures is for Experiment A and the second row of figures is for Experiment B

$$\text{Percentage of trap type in case tested} = \frac{\text{No. of occurrence of trap type in the case investigated}}{\text{Total no. of experiments in the case investigated}} \times 100 \quad (1)$$

2.2 Effect to the flow as a result of trapped TLD by an IFM

For the second objective, a flume channel of 0.7 m wide and 5 m long with a slope of 1/500 was used (Figure 1 b)). Three flow rates producing three different *Fr* were pumped through the channel at a quasi-steady state. The *Fr* when nothing was placed on the flume channel, were 0.65, 0.70 and 0.75. A quasi-steady state experiment was considered to understand the effect of trapped vegetation by an IFM simply.

A model scale of 1/50 was chosen. The IFM spacing (*S*) and the number of rows were investigated. These two factors influenced the trapping function of driftwood (De Costa and Tanaka 2020). Three spacing conditions were considered. They were 0.03, 0.046 and 0.088 m, respectively. Model scale *S* of 0.046 m and a diameter of wooden poles of 0.008 m was based on Japanese black pine (*Pinus thunbergii* Pralat.) in the Sendai region of Japan (Tanaka et al. 2013; Zaha et al. 2019). *S* of 0.03 and 0.088 m spacing were then selected to give a range of different potential spacing conditions. The same diameter, 0.008 m, wooden poles were used for these two spacing conditions. The three *S* values gave *G*/*D* ratios of 0.88, 1.88 and 4.53 respectively. Three different rows were considered. They were 2, 4 and 6 rows in the IFM, respectively.

A model scale conifer plant (*Juniperus Chinensis* Linnaeus) was used to represent the driftwood model (Figure 1 b)). The driftwood models used had an approximate height of 0.2 m, a maximum crown width of 0.07 m in and a trunk height of 0.04 m. The H_{ND} of all the driftwood model used in this experiment was approximately 0.2. The driftwood models investigated had a specific gravity of approximately 1, where specific gravity in a real scenario is around 1 (Tanaka and Ogino 2017)). In a tsunami event, TLD could undergo damage. This study assumed that no damage occurred to the TLD.

The motion of TLD before trapping could take different forms. The TLD could be intertwined or travelling close to each other. However, for better understanding, the driftwood model was released at approximately 2 m upstream of the IFM one at a time, with an approximate one second interval time between the release of the driftwood models. Driftwood was released at the centre of the flume channel, with its long axis aligned to the streamlines (0° to the streamwise condition).

After the trapped driftwood reached stable trapping, the flow depth was measured by using a point gauge. Due to the 3D nature of the flow, the flow depth was measured transversely and longitudinally. Measurements were taken at 0.05 by 0.1 m squares, for approximately 0.6 m downstream of IFM. Each experiment was then repeated three times, to account for the variation in the trapping. The change in flow depth before and after trapping was then calculated. The difference in the flow depth indicates a change in the fluid force index (U^2h) and moment index (U^2h^2) (U is the depth-averaged velocity, and h is the flow depth). Fluid force index and moment index are variables used to understand the damage potential onto structures (Tanaka et al. 2014). Continuity equation ($Q = UA$, where Q is the flow rate and A is the cross-sectional area of flow), and the principle of conservation of mass was used to understand the depth-averaged velocity of the flow. Therefore, it is noted that the fluid force index is proportional to the inverse of flow depth.

3. RESULTS

3.1 IFM as a trapping function

Three different trapping types were noted. They were classified as Type Br - branches getting caught in the trunk, Type PR - partial rotation before two or more trunks, prevented the driftwood from flowing downstream and Type FC - trapping at the front face of IFM in a cross-stream position by one or more trunk(s) (Figure 2)(De Costa and Tanaka 2020). Additionally, the term Type NT was used to represent driftwood not trapped by the IFM.

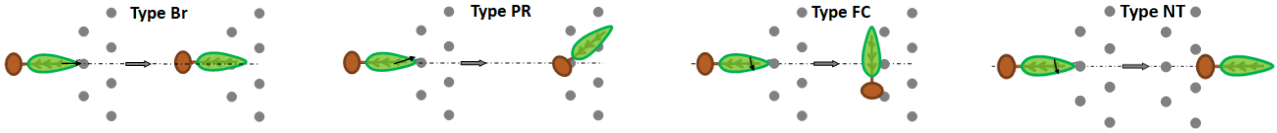

Figure 2: Types of trapping observed, and the non-trapped scenario

3.2 Influence in the *G*/*D* ratio

The trapping function of an IFM changed with driftwoods angle to the streamlines, and this function further changed with the changing *G*/*D* ratio (Figure 3 1st row of graphs). As the *G*/*D* ratio was decreased, the trapping function was increased, with Type FC trapping showing an increase in occurrence. Generally, the trap rate and the driftwood's angle before trapping were influenced more by the low *G*/*D* ratio. A *G*/*D* ratio of 10.6 showed no difference, while a *G*/*D* ratio of 6.8 and 3.0 a decreasing trend of Type NT was noticed. Upon impact of the TLD on the IFM, a rotated driftwood model immediately rotated towards the cross-stream angle and got commonly trapped by Type FC (100% of TLD trapped at *G*/*D* of 3.0 and a 90° angle), or less often as Type PR. When the driftwood model was in a rotated position, due to the low chance of the driftwood model's branches being interacted by the IFM, Type Br decreased with increasing in the driftwood's angle.

3.3 Influence in the number of rows

In the scenario of one row of IFM, with the increase in the initiating angle of the driftwood, a decreasing trend in Type NT was observed (Figure 3 2nd row of graphs). When one row of IFM existed, and when the driftwood model was at a 0° angle to the streamlines, the percentage of Type NT was approximately 60%. However, when the driftwood model was approximately at a 90° angle to the streamlines the percentage of Type NT was 40%. When two or more rows in a staggered arrangement existed, the percentage of Type NT was lower than that of in one row of IFM. Moreover, a rotated driftwood model showed a small decrease in the non-trapped scenario with more than two rows of IFM. Two or more rows allowed for Type PR to occur and increased the probability of being trapped by Type Br.

3.4 Tree height to trunk height ratio

The 3rd row in Figure 3 showed that by increasing the trunk height to tree height ratio of the upstream vegetation, there was no noticeable change in the trapping pattern. Increasing the trunk height shifted the centre of gravity of the TLD more towards the tip of the crown. However, the increase seems minor and therefore, no noticeable change in trapping patterns was observed (De Costa and Tanaka 2020).

3.5 Impact force of TLD

To evaluate the difference in impact force between a rotated driftwood model and trapping type, the average, considering all the conditions were calculated. This was normalized by the hydrodynamic loading on the trunk of the IFM before driftwood impact (Figure 4). Fig. 4 shows that 90° angled driftwood has a higher factor of increase than a 0° angled driftwood model. Type Br shows the greatest difference. At 0°, the factor of the increase was approximately 5.5. When the driftwood model was at a 90° angle, it was approximately 8.0. In the 90° angle, trapped Type Br was observed. In this scenario, one trunk in the IFM was being pulled by the branches of the driftwood model. Since the driftwood model was at a 90° angle, there was a large drag force that the trunk had to support. While when the driftwood was in a 0° or a 45° angle, the driftwood was trapped in a near streamwise direction.

Similarly, Type FC trapping had a factor of increase of 7 when driftwood was at a 0° angle before impact and had a factor of increase of 7.8 when it was at a 90° angle before impact. Type Br and Type FC had the largest factor of increase of approximately 8 and 7.8 when it was at a 90° angle before impact.

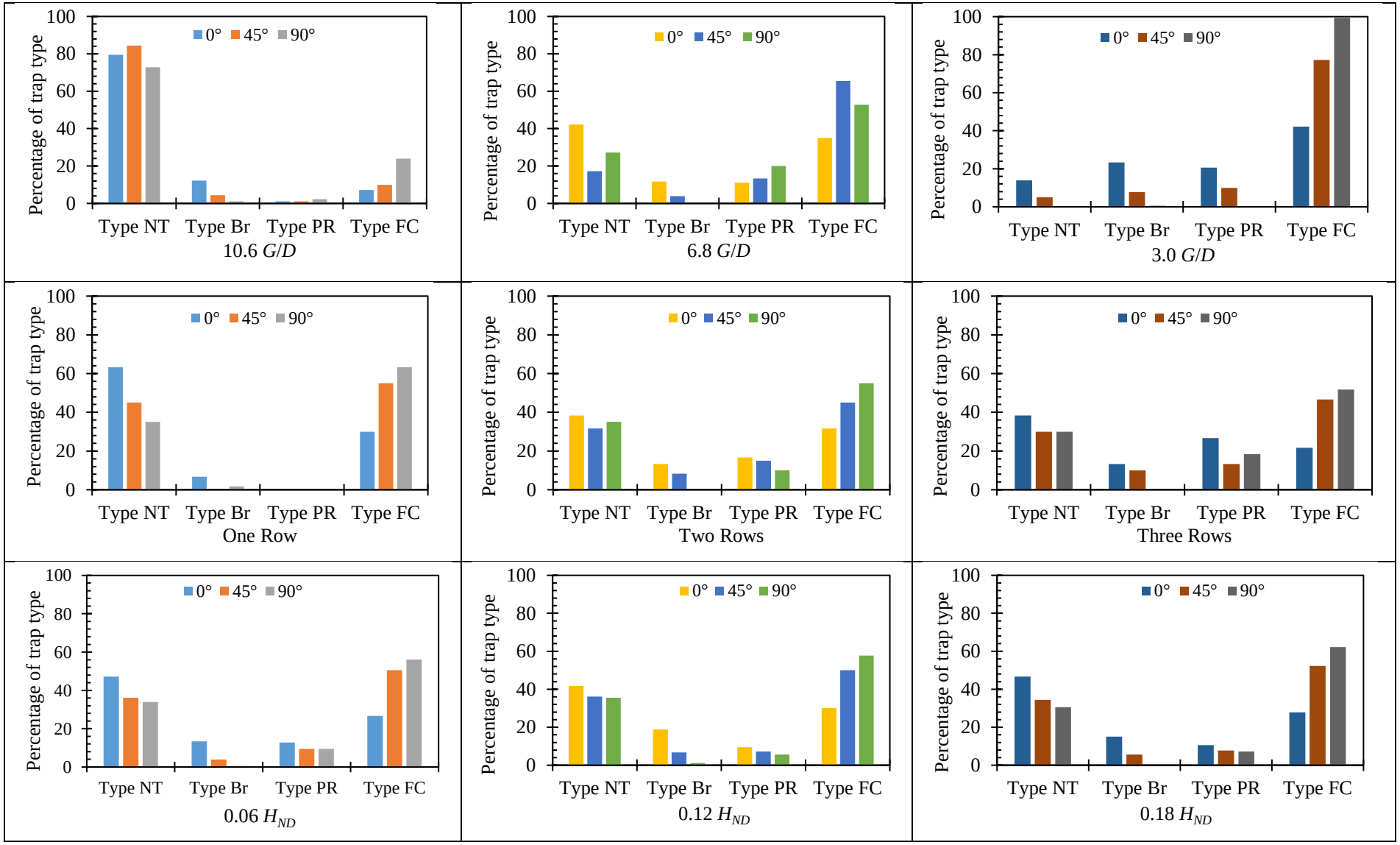

Figure 3 Trapping rate with IFM conditions 1st row) Varying *G*/*D*, 2nd row) Number of rows and 3rd row) Tree height to trunk height ratio (H_{ND})

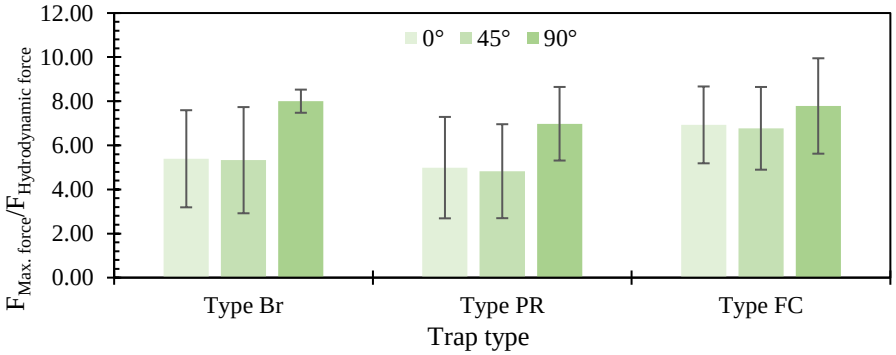

Figure 4 Change in the average maximum force due to change in the driftwoods angle before trapping by the IFM

3.6 Effect of driftwood trapping onto the flow

The second flume channel experiment showed that, as the driftwood models were added onto the flume channel, the initial driftwood assisted in trapping the other driftwood models. As driftwood was added into the flume channel, the driftwood collided with the already trapped driftwood and rotated where the long axis of the driftwood was perpendicular to the direction of flow. It would then move and fill the nearby open spaces at the front face of the IFM. This was due to the greater velocity within open spaces pulling the driftwood model towards it. The trapped driftwood then reduced the porosity at the front face of the IFM. This altered the upstream and downstream flow.

Upstream saw a near-uniform increase in flow depth with a small ripple formation close to the trapped driftwood models. Downstream of the IFM, the trapped vegetation created a horse-shoe type flow formation, with the region just directly behind the trapped driftwood models, having a higher flow depth than the areas to the side of it (Figure 5). It was observed that as driftwood accumulated, the horse-shoe formation moved closer to the downstream face of the IFM.

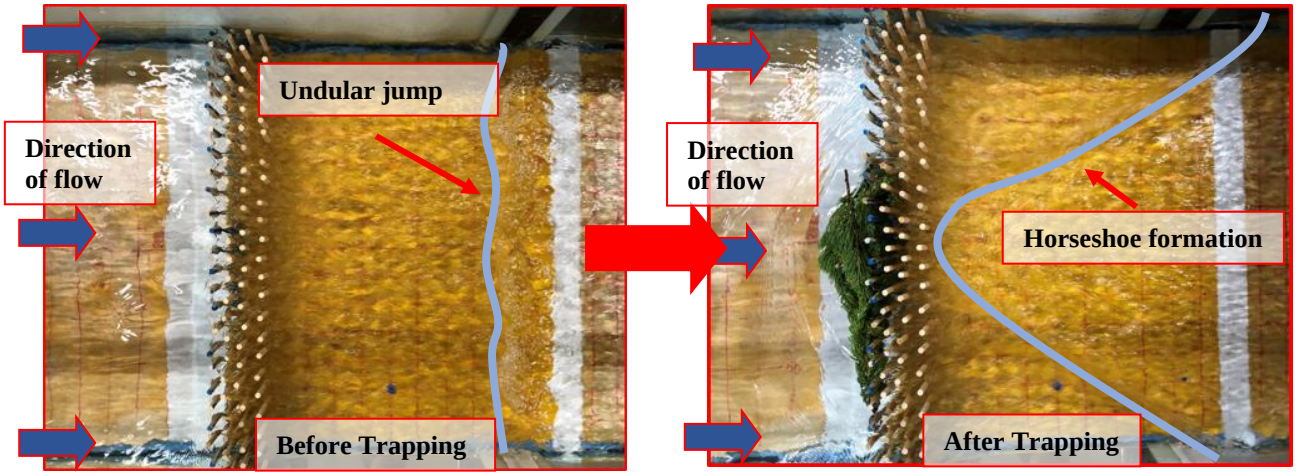

Figure 5 Effect of driftwood trapping to the flow (IFM is 0.88 *G*/*D* and four rows)

The *G*/*D* ratio and the number of rows within the IFM have different effects on both the upstream and downstream flow of an IFM that has trapped driftwood. Figure 6 shows the ratio of the average flow depth upstream (h_{TDU}) and downstream (h_{TDD}) of an IFM that has trapped TLD versus the initial flow depth before trapping of TLD upstream (h_U) and downstream (h_D), respectively.

Figure 6 a) and b) shows that small *G*/*D* ratio (dense condition) and a high number of rows in the IFM had a lesser effect on the upstream flow depth of an IFM that has trapped driftwood. The change in the porosity at the front face of the IFM with *G*/*D* ratio of 0.88, after trapping of driftwood was minor. Therefore, the change in the upstream flow depth was minor. The higher the number of rows the lesser the effect of trapping to the upstream flow. Due to the significant change in the porosity of the IFM, after trapping in high *G*/*D* ratios, the effect to the flow upstream of the IFM was more noticed. With increasing in *Fr*, the effect of trapped TLD by an IFM on to the incoming flow decreased.

Figure 6 c) and d), shows that with high *G*/*D* ratio condition (sparse condition) and a high number of rows, the effect of the trapped vegetation onto the downstream flow is low. While, low *G*/*D* ratio condition (dense condition) and only a few rows of trees, show a more significant change to the downstream flow depth. This decrease in trend implies an increase in the fluid force index. As *Fr* increased *G*/*D* of 0.88 show a further reduction in change in the flow depth, while larger *G*/*D* does not indicate that. This no change in the flow

depth also indicates that there is minor to no effect of trapped driftwood by an IFM on the flow in high *G/D* values, in high *Fr* scenarios. However, low *G/D* values are encouraged to ensure a higher trapping rate of driftwood.

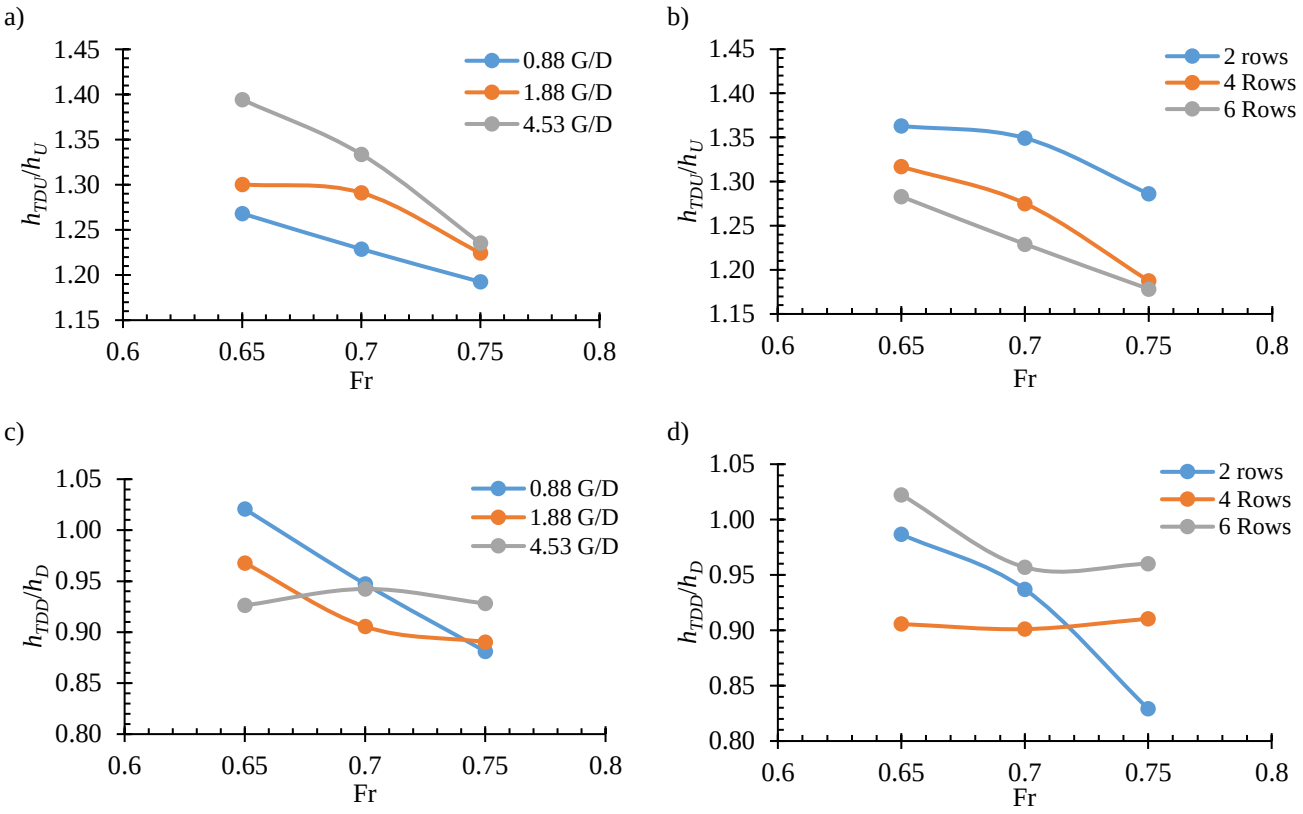

Figure 6 First row of graphs: Change in the upstream flow depth a) *G/D* b) Number of rows; the second row of graphs: change in the downstream flow depth c) *G/D* d) Number of rows

4. DISCUSSION

A rotated driftwood model increased the trapping function of an IFM. Placing an embankment and moat structure, as discussed by De Costa et al. (2019), rotated a driftwood model. A hybrid structure that consists of vegetation, embankment and moat, not only increases the energy dissipation (Zaha et al. 2019) but induced rotation that, as shown by this study, can later encourage the trapping function of an IFM. However, since a rotated driftwood model showed, on average, a slightly larger maximum force than an un-rotated driftwood model, this needs to be considered when designing an IFM, i.e. be designed for a 90° angled TLD's maximum force. This design consideration could include, choice of vegetation species and required minimum d_{BH} (diameter at breast height) (De Costa and Tanaka 2020). It should be noted that, once one TLD is trapped it assists in trapping further TLD.

A successfully designed IFM prevents impact by TLD onto downstream structures. It can be argued that the trapped TLD acts to constrict the flow of an IFM and, therefore, region downstream of trapped TLD increases in velocity. This increase in velocity increases the fluid force index and therefore puts structures downstream of trees trapping driftwood in danger. To better design an IFM to consider this into account, a lower *G/D* ratio (higher trapping function), with many rows are required to ensure this effect is low. Moreover, IFM with trapped driftwood, can then further dissipate energy and further reduce the forces acting on the structures downstream of the IFM.

5. CONCLUSIONS

An IFM shows strong capability in trapping TLD. A rotated driftwood model, before impact by the IFM, increased the trapping function of the IFM. This trapping function is especially noticed in an IFM with low *G/D* values. This study showed that increasing the number of rows and changing the H_{ND} had no noticeable effect on a rotated driftwood model before impact and the trapping function. Moreover, an increase in average maximum force was measured between a non-rotated driftwood model and a rotated driftwood model. The design of an IFM will need to consider this increase in force to ensure safe trapping.

When the TLD got trapped by the IFM, the flow condition downstream of the IFM changed. The change in the IFM properties and the *Fr* of the flow changed the effect of trapped TLD to the flow. High *G/D* ratio saw

on average, less change, and increasing the number of rows saw a decrease in the effect of change in the average flow depth downstream of the IFM.

Therefore, an inland forest can be designed not only to reduce the tsunami wave forces and prevent tsunami-related driftwood impact forces but also to reduce the effect of this constricted flow. Further study includes investigating the change in erosion behaviour around an IFM as a result of trapped TLD by an IFM.

REFERENCES

De Costa R, Iwata A, Tanaka N (2019) Tsunami Generated Large Wooden Debris Movement Considering Hybrid Structures. Japan Soc Civ Eng (Hydralulic Eng 75:727–732

De Costa R, Nandasena NAK (2018) Pohutukawa bio-shield on the coast of New Zealand as a tsunami mitigation strategy Pohutukawa bio-shield on the coast of New Zealand as a tsunami mitigation strategy. Eur J Environ Civ Eng 0:1–12. https://doi.org/10.1080/19648189.2018.1494635

De Costa R, Tanaka N (2020) Inland forest as a trapping function against tsunami-borne large broken or washed out trees. Landsc Ecol Eng. https://doi.org/10.1007/s11355-020-00408-9

Felisa G, Ciriello V, Di Federico V (2013) Saltwater intrusion in coastal aquifers: A primary case study along the adriatic coast investigated within a probabilistic framework. Water 5:1830–1847. https://doi.org/10.3390/w5041830

Haehnel RB, Daly SF (2004) Maximum impact force of woody debris on floodplain structures. J Hydraul Eng 130:112–120. https://doi.org/10.1061/(ASCE)0733-9429(2004)130:2(112)

Imai K, Hayashi A, Imamura F (2018) Evaluation of the ability of lines of trees to trap tsunami flotsam. Coast Eng J 60:308–317. https://doi.org/10.1080/21664250.2018.1520795

Marois DE, Mitsch WJ (2015) Coastal protection from tsunamis and cyclones provided by mangrove wetlands - A review. Int J Biodivers Sci Ecosyst Serv Manag 11:71–83. https://doi.org/10.1080/21513732.2014.997292

Natuhara Y (2018) Green infrastructure: innovative use of indigenous ecosystems and knowledge. Landsc. Ecol. Eng. 14:187–192

Pasha GA, Tanaka N (2016) Effectiveness of finite length inland forest in trapping tsunami-borne wood debris. J Earthq Tsunami 10:1650008-1~1650008-26. https://doi.org/10.1142/S1793431116500081

Schmocker L, Hager WH (2013) Scale modeling of wooden debris accumulation at a debris rack. J Hydraul Eng 139:827–836. https://doi.org/10.1061/(asce)hy.1943-7900.0000714

Stolle J, Takabatake T, Nistor I, et al (2018) Experimental investigation of debris damming loads under transient supercritical flow conditions. Coast Eng 139:16–31. https://doi.org/10.1016/j.coastaleng.2018.04.026

Takemura T, Tanaka N (2007) Flow structures and drag characteristics of a colony-type emergent roughness model mounted on a flat plate in uniform flow. Fluid Dyn Res 39:694–710. https://doi.org/10.1016/j.fluiddyn.2007.06.001

Tanaka N, Ogino K (2017) Comparison of reduction of tsunami fluid force and additional force due to impact and accumulation after collision of tsunami-produced driftwood from a coastal forest with houses during the Great East Japan tsunami. Landsc Ecol Eng 13:287–304. https://doi.org/10.1007/s11355-016-0321-7

Tanaka N, Onai A (2017) Mitigation of destructive fluid force on buildings due to trapping of floating debris by coastal forest during the Great East Japan tsunami. Landsc Ecol Eng 13:131–144. https://doi.org/10.1007/s11355-016-0308-4

Tanaka N, Sato H, Igarashi Y, et al (2018) Effective tree distribution and stand structures in a forest for tsunami mitigation considering the different tree-breaking patterns of tree species. J Environ Manage 223:925–935. https://doi.org/10.1016/j.jenvman.2018.07.006

Tanaka N, Suzuki I (2013) Comparison between Drag Force on a House behind Coastal Forest and Impulsive Force by Tsunami-driven Woody Debris from the Forest at the Great East Japan Earthquake. In: Proceedings of the 35th Iahr World Congress, Vols Iii and Iv

Tanaka N, Yagisawa J, Yasuda S (2013) Breaking pattern and critical breaking condition of Japanese pine trees on coastal sand dunes in huge tsunami caused by Great East Japan Earthquake. Nat Hazards 65:423–442. https://doi.org/10.1007/s11069-012-0373-4

Tanaka N, Yasuda S, Iimura K, Yagisawa J (2014) Combined effects of coastal forest and sea embankment on reducing the washout region of houses in the Great East Japan tsunami. J Hydro-Environment Res 8:270–280. https://doi.org/10.1016/j.jher.2013.10.001

Thuy NB, Tanaka N, Tanimoto K (2012) Tsunami mitigation by coastal vegetation considering the effect of tree breaking. J Coast Conserv 16:111–121. https://doi.org/10.1007/s11852-011-0179-7

Udo K, Sugawara D, Tanaka H, et al (2012) Impact of the 2011 Tohoku earthquake and tsunami on beach morphology along the northern Sendai coast. Coast Eng J 54:1250009-1-1250009–15. https://doi.org/10.1142/S057856341250009X

Zaha T, Tanaka N, Kimiwada Y (2019) Flume experiments on optimal arrangement of hybrid defense system comprising an embankment, moat, and emergent vegetation to mitigate inundating tsunami current. Ocean Eng 173:45–57. https://doi.org/10.1016/j.oceaneng.2018.12.054